

Article

**Characterization of Different Biochars Produced and Compositated
with Nano Silver Prepared by Eco-friendly method**

**Fatima Namir Awaad*¹, Abdulqadier Hussien Al khazraji¹, Alaa
Hasan Fahmi²**

¹Department of Chemistry, College of Education for Pure Science, University of Diyala, Iraq.

²Department of Soil Sciences and Water Resources, College of Agriculture, University of
Diyala, Iraq

Corresponding Author fatma89480@gmail.com

Abstract

An environmentally friendly and economical material, biochar has drawn great attention to soil and wastewater remediation. However, its properties and behaviors for adsorption pollutants are different depending on feedstock and pyrolysis conditions. This study prepared biochar from different feedstocks (wheat straw and walnut shells) at different temperatures (300 and 600 °C), and composite with nano silver oxide. Nano silver oxide was prepared by using the green method. The obtained biochar with/without nano silver coating was then characterized using XRD, FESEM, etc. The results showed that the nano-size of the silver nanoparticles was about 56.44 nm. Biochar was found to contain organic elements such as carbon, hydrogen, sulfur, and nitrogen. For composite biochar with nanosilver, the XRD result confirmed the Nano silver-coated biochar. FE-SEM examination for silver oxide showed the surface image in the form of silver spheroids with an average size of 41.8 nm. For biochar with increasing temperatures, the surface went from rough to smooth, and its porosity increased. The FE-SEM confirmed the nanosilver was distributed over the channels within biochar. The results of EDX showed biochar consists of a wide range of organic and inorganic elements. The percentage carbon content increased with temperature

increased and within walnut shells was higher than the wheat straw feedstock. The BET surface area results showed that walnut shells biochar had a higher value than the wheat straw biochar and value with increasing pyrolysis temperature from 300 to 600 °C, which were 10.44, 210.07, 1.1959 and 80.251, respectively. However, all biochar composited with nanosilver led to a reduction in surface area. The carbon content in biochar increased with increasing temperature pyrolysis, and the biochar produced from wheat straw had higher carbon content than the biochar of walnut shells, as well as reduced in biochar composites with nano silver. Therefore, the adsorption capacity of these materials for pollutants could be differentiated based on these properties. The biochar for wheat straw at 300 and 600 had a nano size of 152 nm, and at a temperature of 600 °C, it had a nano image and size of 34 nm. For Walnut shells, It was 300 and 600 images. It has a nano size of 26 600 shapes and a size of 28,134.

Keywords: Biochar, Pyrolysis, Plant extract, Nanosilver, Walnut shells, wheat straw

Introduction

Biochar is a by-product containing a large percentage of carbon that is produced by heating the mass during the pyrolysis process in an oxygen-free environment [1]. It can also be formed from all types of natural wastes and thus have different chemical and physical properties under different conditions of pyrolysis. Biochar contains a composition of organic matter. They range from barely decomposed lignin at low temperatures to a Highly carbonized material at high temperature and coke containing it is formed by the interaction of volatile components, Previous studies indicated this [2]. Through pyrolysis, a coal containing carbon that is highly resistant to decomposition is formed. The porosity and surface area depend on various factors: temperature, heating rate, pressure, and ash content. Micro pores are formed in biochar at high temperatures. Many studies have been conducted on preparing biochar composites with nano-oxides in different ways to increase biochar's effectiveness, including (surface properties, more stability, active sites, and more porosity). Which enhances the possibility of simultaneous adsorption and decomposition of multiple pollutants in water, Previous studies indicate [3] The discovery of nano-silver oxide among nano-metals attracted silver nanoparticles that have been used since the 1880s. Silver nanoparticles have a large surface area and, as a result, provide high surface energy and many sites for interaction. These properties make silver nanoparticles more catalytic than

other materials, and many physical and chemical green synthesis methods exist. One of these methods is the rapid biosynthesis of silver nanoparticles to obtain nanoparticles. Through the chemical flame deposition method, the growth of crystals at low temperatures is controlled by About 90 °C. The nano silver was manufactured from a plant source to be used in several applications and to study the characteristics of the product in different ways.

Therefore, this study aims to prepare nano silver oxide in an environmentally friendly method and prepare biochar from different feedstocks at different temperatures. Then, a binary composite of nanosilver oxide with biochar was prepared by the solution treatment method.

Materials and Methods

Feedstock Sources and Pyrolysis

Walnut shells (WSH) and wheat straw (WST) samples were collected from the Bahquba – Diyala - Iraq field. Samples were left to dry and then crushed. For producing biochar, the samples were put into ceramic crucibles with covers and then placed into a furnace muffle (Daihan Labtech oven, LDO-60e, South Korea) to pyrolysis at (300 and 600 °C) for 2 h. The biochars produced were signed as (WSHB300, WSHB600, WSTB300 and WSTB600). All biochars were crushed and passed through the sieve <50 µm according and left for prior analysis, As in previous studies[4]. The calculation of the biochar yield was according to the following equation.

$$\text{Biochar Yield (\%)} = \frac{\text{weight of biochar (g)}}{\text{feedstock dried weight(g)}} \times 100\% \text{ ----- (1)}$$

Preparation of plant extract

20 grams of (Melia azedarach plant) were weighed in 100 mL of non-ionic water in a 200 mL beaker on a hot plate device at a temperature of 80 °C Previous studies indicate, stirring for three hours. A brown extract was formed, and it was filtered from contaminants and leaves and then placed in a glass container to be kept and cooled in the refrigerator for use later, Previous studies indicated this[5]. Figure 1 shows the process of producing the plant extract.



Figure 1. Steps to prepare a plant extract.

Preparation of nanosilver oxide (Ag₂O) by the green method

The nanomaterial was prepared by taking 3 g of silver nitrate and dissolving it in 20 mL of nonionic water in a 50 mL beaker. The beaker was placed on a hot plate device. 10 mL of the plant extract (Melia azedarach plant) was added using the burette drop by drop to the dissolved silver nitrate until the color changed and became a light black. At the same time, 10 mL of sodium hydroxide base solution was added from the burette drop by drop until the solution became basic at a pH of 12, and the color began to change to dark brown. The temperature gradually rises to 80 °C, and the process continues stirring for an hour. A precipitate was formed and then filtered using filter paper. The precipitate was washed with ethanol to remove contaminants, then with non-ionic water until obtaining a solution with pH 7. The precipitate was dried using an oven at 80 °C. The dry material was calcined at 500 °C to obtain nano-sized silver oxide, Previous studies indicate [6]

Preparation of Ag₂O/Biochar as binary composite

The binary compounds were prepared by dissolving 0.5 g of nanosilver oxide in 20 mL of ethanol, placed in a 30 mL beaker put in an ultrasonic device. In another beaker, 1 g of biochar (WSHB or WSTB) prepared at two temperatures (300 or 600⁰C) was suspended in 20 mL of ethanol in a beaker volume of 30 mL, then was placed in the ultrasonic device for half an hour at a temperature of 50 °C. After that, the nanosilver oxide suspension was poured into the biochar suspension, and the reaction mixture was then filtered and dried in an oven at 50 °C for two hours to obtain the binary compounds ,Previous studies indicated this[7], as shown in Figure 2.

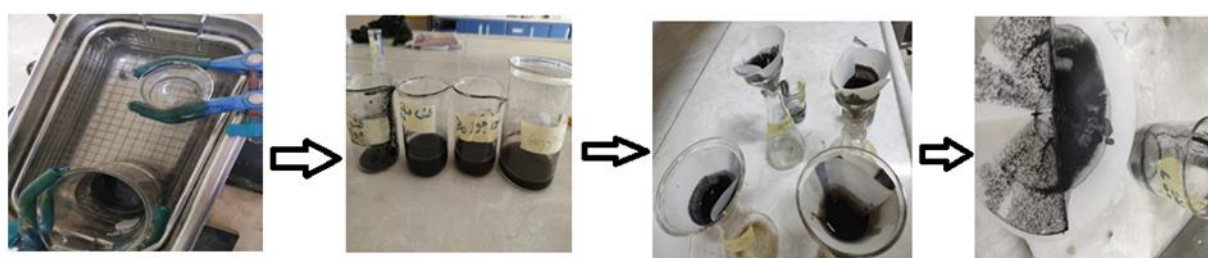


Figure 2. Steps of preparing biochar composite with nanosilver

Characterization of preparing materials

The prepared materials (WSHB300, WSHB600, WSHB300N, WSHB600N, WSTB300, WSTB600, WSTB300N and WStB600N) were characterized. For the following properties:-

pH :The pH was measured for WSHB300, WSHB600, WSTB300 and WSTB600 WSHB300N, WSHB600N, , WSTB300N and WStB600N biochar[8]. 4.0 grams of each biochar was mixed

with 100 millilitres of water in a conical container. The beaker was covered while it boiled for 5 minutes, then the mixture was left to cool, and the pH was measured.

Electrical Conductivity (EC) The electrical conductivity was measured by taking 1 gram of biochars and adding 5 mL of water and shaking for 24 hours. The measurements were made for each of the following WSHB300N, WSHB600N, WSTB300N and WStB600N.

Ash content The ash content in biochar was measured by the dry combustion method by heating about 5.0 grams of biochar at a temperature of 500 °C for 8 hours [9]. The ash content was then cooled at room temperature and the material was weighed and calculated by the following equation

$$\text{ASH content \%} = (\text{ASH weight} / \text{weight of biochar}) \times 100$$

CHNS analysis: The elements were analyzed, and different results appeared for the percentages of carbon, hydrogen, nitrogen, and sulfur.

Field-Emission Scanning Electron Microscopy (FESEM): Surface morphology analysis of all biochar samples using field emission scanning electron microscopy.

X-ray diffraction analysis (XRD): Samples with different particle sizes of biochar were examined using an advanced Bruker D8 X-ray diffraction. Samples were prepared by placing powder in the sample holder. The sample holder was then arranged in a diffraction with a voltage of 40 kV, and samples from 20 to 100 were examined at a speed of 1 per minute.

Element content

The element's content in the samples was determined according to the method [10].

Surface area (SA)

The surface area of the biochar, Ag₂ONp, and composite samples was determined by N₂ adsorption at 77 K; prior to the analysis, the biochar samples were degassed at 200 °C for 9 hours. The multipoint BET method was used to calculate the total surface area. The t-plot method was used to calculate the micropore surface area. The pore volumes were determined from their desorption isotherms. The total pore volume was determined using a single N₂ adsorption point at a P/P₀ of 0.97.

Results and Discussion

X-ray diffraction analysis

A- XRD result of silver oxide nanoparticles

The average crystal size appeared to be 56.44 nm, and its peaks appear at different angles: 40°, 65°, 79°, and 38° for Silver Oxide nanoparticles, as shown in Figure 3. As in previous studies [11-13].

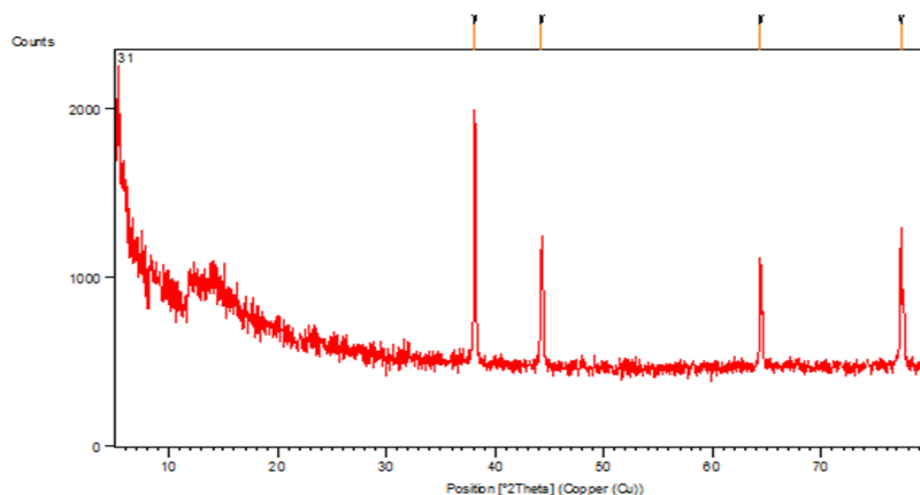


Figure 3. XRD of Silver Oxide nanoparticles

B- XRD result of biochar

Biochar of wheat straw prepared at 300 °C (Figure 2 A) was analysed. It was found that a sharp peak appeared at an angle of 28°, which means the presence of organic elements, such as carbon, in a large percentage and the rest of the elements, such as hydrogen, sulfur, and nitrogen, in a smaller percentage. The average size of its crystals was calculated and was up to 63.5 nm. It was noticed from Figure 2 B (600°C) shows the appearance of many peaks with increasing temperature due to the appearance of a number of elements ,Previous studies indicate[14], where the clearest peak was at 28°, and the average nano size was 41.25 nm. Meanwhile, walnut shells have biochar at 300 °C and 600 °C, as shown in (Figures 2 C), andD, respectively. The X-ray spectrum showed clear peak angles of 31°, with an average crystal size of 264 nm. Figure 2 D shows an increase in the angles and the number of peaks, where the highest peak was 31°, and its average nanosized was 35 nm due to increasing the temperature of the prepared biochar, Previous studies indicate[15].

XRD result of biochar composite with nano silver oxide

In Figure 2 E, the X-ray spectrum of the wheat straw biochar nanocomposite at 300 °C showed a peak at an angle of 38° and another angle at 44°, which indicates the structure of silver oxide. Its

average crystal size was 44 nm. However, with wheat straw biochar nanocomposite at 600 °C, the crystal size appeared to increase, reaching 55 nm (Figure 4 F).

In Figure 2 G, the X-ray spectrum of the prepared substance shows a difference in the peaks for each of them, indicating the presence of several organic elements such as carbon, hydrogen, and sulfur. Peaks appeared for the raw material samples at an angle of 31°, with an average nanometer size of 35.6 nm.

In Figure 2 H, when the temperature of the prepared material was increased (600 °C), there was a noticeable change in the location of the peak and a decrease in the carbon percentage at an angle of 8°, with an average nano size of 22.5 nm.[16]

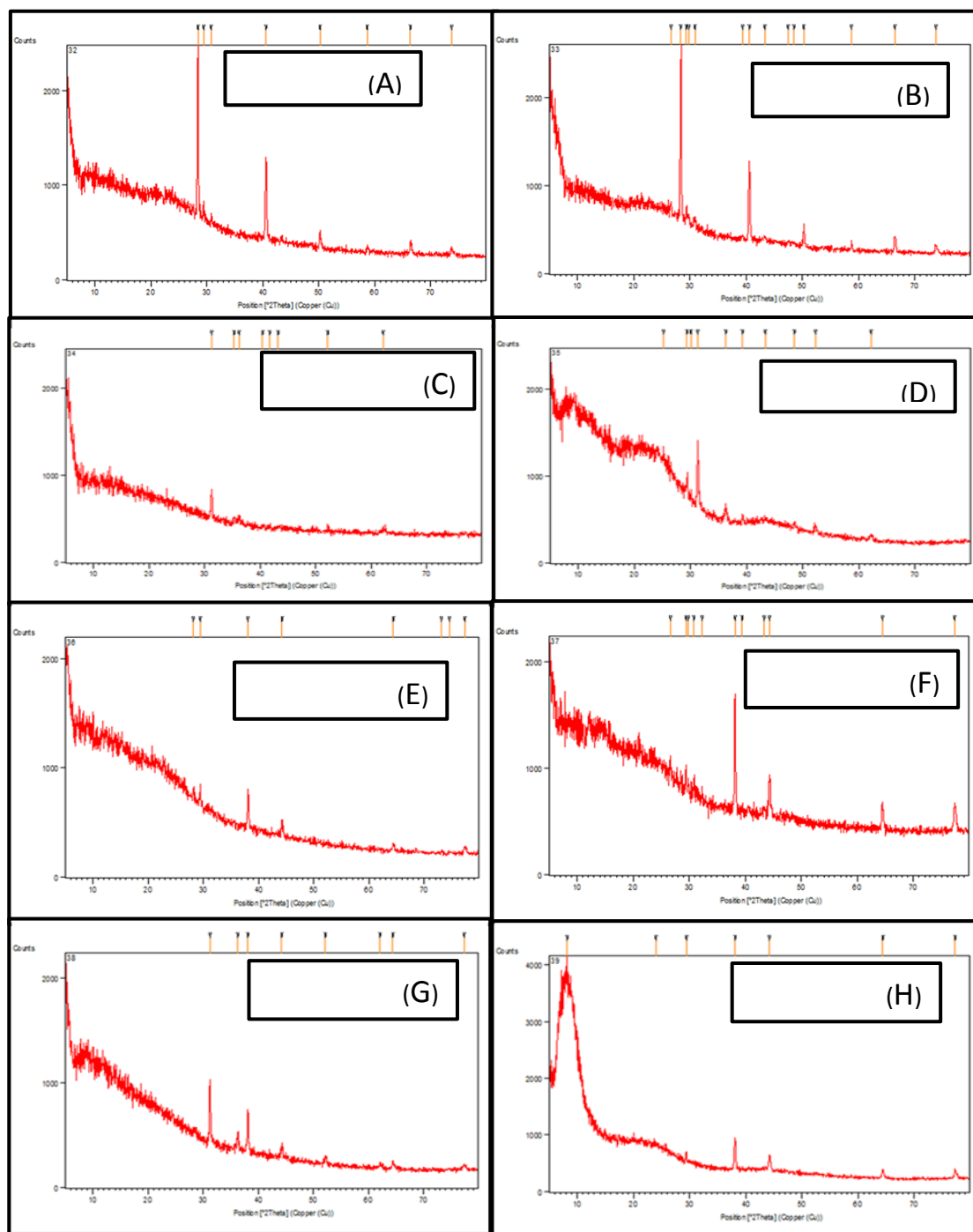


Figure 4. XRD of wheat straw biochar at 300 °C (A) and at 600 °C (B), walnut shells biochar at 300 °C (C) and at 600 °C (D), Wheat straw biochar composite with silver oxide at 300 °C (E) and at 600 °C (F) and walnut shells biochar with nano silver oxide at 300 °C (G) and at 600 °C (H).

Field-Emission Scanning Electron Microscopy of the prepared biochars (FESEM):

A- Nano silver oxide Ag₂O

In the following Figure 5, an electron microscope image of silver oxide nanoparticles shows its appearance as a spherical aggregate with a nano-size of 24 nm and an average size of 41.8 nm, Previous studies indicated this[17]. This result was in line with the previous result of XRD.

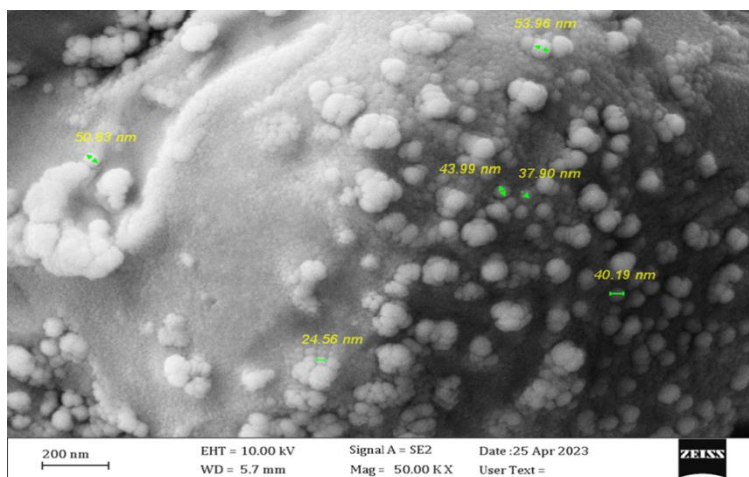


Figure 5. FESEM of Nanosilver oxide Ag₂O

B- biochar

The following Figure (6A) shows an electron microscope image of biochar from wheat straw300. It had a stick-like shape, and ovoid particles spread randomly on the surface. The nano size was 237.5 nm, and the average nano size was 152 nm. the picture of porosity change in coal appears in Figure (6B). It showed the formation of shapes as a result of the increase in temperature [18], as the size became smaller and stuck together and reached 15 nm compared to the previous size, and the average nano size was 34 nm. Biochar from walnut shells 300 °C and 600 °C. The following Figure (6C) shows an electron microscope image of biochar from walnut shells 300, showing surface roughness and the formation of numerous channels and pits, Previous studies indicated this. The average nanopore size was 26 nm. As the temperature increased in Figure (4D), the surface went from rough to smooth, and its porosity increased, Previous studies indicated this [19] as its crystal size became medium 28.134 nm.

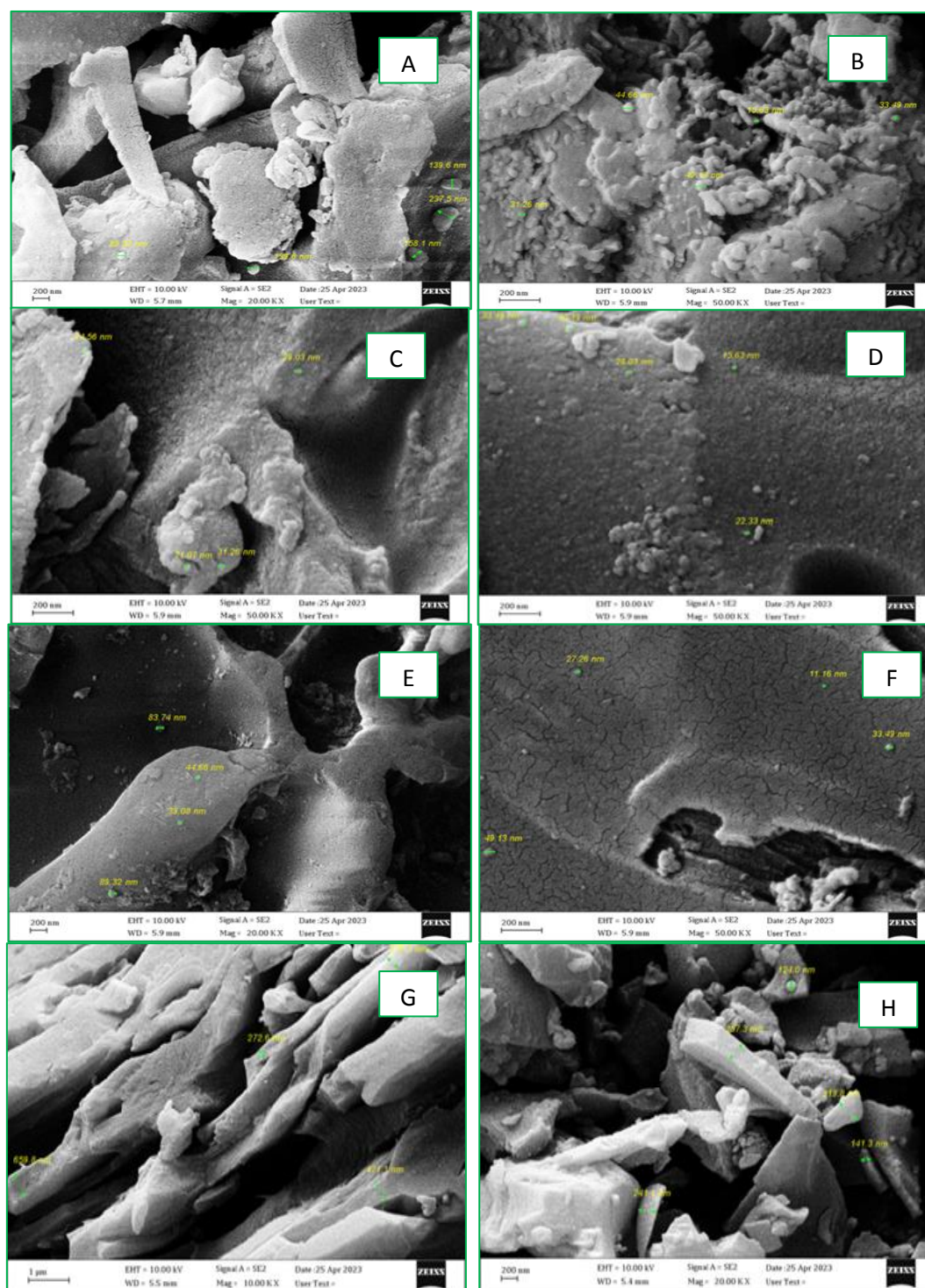


Figure 6. FESEM of wheat straw biochar at 300 °C (A) and at 600 °C (B), walnut shells biochar at 300 °C (C) and at 600 °C (D), Wheat straw biochar composite with silver oxide at 300 °C (E) and at 600 °C (F) and walnut shells biochar with nano silver oxide at 300 °C (G) and at 600 °C (H)

Silver oxide composited with biochar from wheat straw and walnut shells at 300°C and 600

The following Figure (6E) shows an image of a composite of wheat straw 300 °C. Its surface was rough and untidy and contained large channels. The silver was distributed over the channels in the form of a white sheet, and its average nano size was 64 nm. In comparison to the following Figure (6F), we notice that when the temperature increased, the shape became regular and smooth and did not contain channels, and small-sized silver oxide particles spread on the surface, where the average nano size was 30 nanometers[20] [21][22][23] . The following Figure (6G) shows an electron microscope image of an overlay of walnut shells 300, and we notice stick-like shapes in it, with a large nano size of 659.8 nm. It was larger than silver oxide, which appeared small, and the average nano size appeared to be 467 nm. The other Figure (6H) shows an electron microscope image of a composite of prepared walnut shells 600 °C. As the temperature increases, plate-like shapes appear, on the one hand, spherical ones, belonging to silver oxide, and on the other hand, stick-like, with a nano-size of 257 nm, and the average nano-size measurement was 216 nm

Energy-dispersive X-ray spectroscopy of silver oxide nanoparticles

The following Figure 7 shows the EDX of silver oxide nanoparticles prepared by the green method. Here we notice the decomposition of the basic elements that make up the compound, Previous studies indicated this[24]. The percentage of silver was 95% and the percentage of oxygen was 1.7%

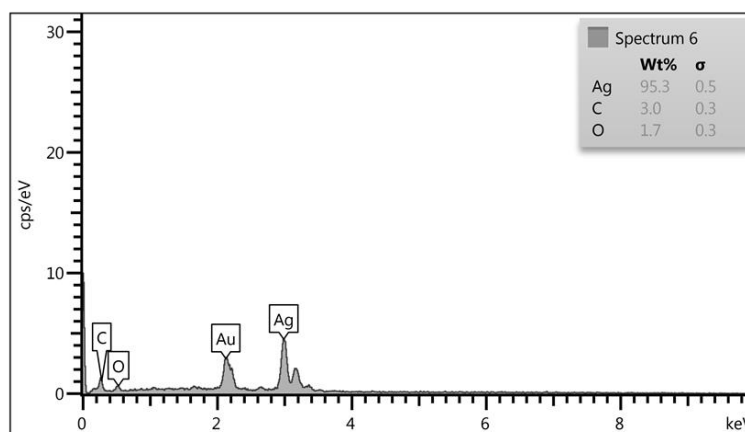


Figure 7. EDX scattering X-ray microscope of silver oxide nanoparticles

EDX for biochar from wheat straw and walnut shells at 300 °C and 600 °C

Biochar consists of a wide range of organic and inorganic elements, which are considered the main components of biochar despite the different feedstocks. The following Figure (6A) shows the scattering X-ray spectrum of biochar from wheat straw at a temperature of 300°C, where the percentages of the analysed elements of these materials were as follows: Carbon 35% constitutes the largest percentage of biochar, followed by oxygen 25%, then calcium 19%. The rest of its components are (sulfur, potassium, chlorine, and magnesium), which constitute small percentages of them. As for Figure (6B) showing the spectrum of scattered rays at a temperature of 600 °C, there was a noticeable change in the proportions of the elements that make up carbon, as it increased to 36.7%, and a significant decrease in the rest of the elements, such as oxygen and calcium[25][26][27][28]. The following Figure (6C) shows the dispersion radiation analysis of the components of biochar, which comes from walnut shells, at a temperature of 300°C the percentages of its components were as follows: carbon was 77.7%, oxygen was 15.4%, while the remaining elements, such as potassium and calcium, were in very low percentages[29] .

When the temperature rose to 600 in Figure (6D), all the existing carbon was transformed into biochar. Because the percentage of carbon was high,

Silver oxide composited with biochar of wheat straw and walnut shells at 300 °C and 600 °C

The following Figure (8e) gives an image of a composite of wheat straw 300 °C in the form of spreading peaks with nanoscopic dimensions of 1.8µm, 6nm.

The following Figure(8f)shows an image of a composite of wheat straw 600°C, shaped like spike peaks, with nanoscopic dimensions of 1.4µm, 10nm. Over layed walnut shells 300 °C and 600 °C, The following Fig.(8g) gives the shapes of an overlay of walnut shells 300 °C, peaks distributed unevenly, with a thickness of 1.8 µm and a height of 2.5 nm.

The following Figure (8h) shows the material formed as a result of the increase in temperature at 600 °C. It gave an even distribution of the material, and the dimensions of the plate appeared at 8n m and a thickness of 1.4µm

BET surface area

To analyze the surface area of the prepared materials, adsorption and desorption isotherms of nitrogen gas (N₂) were used at a temperature of (77 K). The specific surface area of the data using adsorption was calculated from the linear portion of the adsorption isotherm of the gas (N₂) using BET. Surface characterization of the prepared nanoparticles based on the N₂ adsorption isotherm showed differences the working surface as well as the compositional wats, as shown

in Table (1). The wheat straw sample prepared at a temperature 600 °C showed a large and large surface area. It reached (210.07 m² g⁻¹) and the pore volume was (0.1004 cm³ g⁻¹) with high pore diameters of (1.9121 nm) according to the analysis of the data in Table (1-4). Followed by walnut shells prepared at (600 °C), which gave a good surface area (asBET) as well, reaching (80.251 m² g⁻¹)[30][31] . On the one hand, the temperature of the two types of biochar had a clear and positive effect on the surface area. We note from Table (1) that the prepared binary composites gave small surface areas compared to the biochar alone, as the overlay of silver oxide nanoparticles with them did not improve the surface area of the biochar prepared at both temperatures. Rather, the role of secondary silver oxide was negative and reduced the surface area of the biochar.

Table(1):Analysis of BET data for prepared models

Average pore diameter [nm]	Total pore volume[cm ³ g ⁻¹]	BET [m ² g ⁻¹]	Sample
11.533	0.0065536	2.273	Ag ₂ O
13.399	0.034971	10.44	Wheat Straw Biochar300 ⁰ C
1.9121	0.1004	210.07	Wheat Straw Biochar600 ⁰ C
12.616	0.0037721	1.1959	Walnut shells Biochar300 ⁰ C
1.8196	0.036507	80.251	Walnut shells Biochar600 ⁰ C
81.054	0.015293	0.75473	Composite nanosilver with Wheat Straw Biochar300 ⁰ C
8.5906	0.015271	7.1105	Composite nanosilver with Wheat Straw Biochar600 ⁰ C
11.36	0.021297	7.4986	Composite nanosilver with Walnut shells Biochar300 ⁰ C
11.772	0.018057	6.1358	Composite nanosilver with Walnut shells Biochar600 ⁰ C

CHNS analysis

In general, as shown in Table 4, the results of carbon content increased with increasing temperature pyrolysis, and the biochar of wheat straw had higher carbon content than the biochar of walnut shells, as well as reduced with nano silver biochar composites. The carbon content was 53.51, 55.31, 72.82, 85.03, 17.76, 44.5, 28.85 and 61.18% for WSTB300, WSTB600, WSHB300, WSHB600, WSTB300N, WSTB600N, WSHB300N and WSHB600N,As for hydrogen, their proportions were respectively 4.63, 4.21, 4.5, 4.46, 2.86, 5, 2.52, 5.02%. As for

oxygen was 40.95, 39.64 ,21.8, 9.66, 78.95, 49.74, 68.28, 33.1%. The percentage of nitrogen for each material was respectively 0.9, 0.84, 0.88, 0.85, 0.43, 0.76, 0.35, 0.7.

Result pH and EC

The pH of the wheat straw was measured the result at 300 and 600,8.94,12.00, and measurement of both walnut shells was 300 and 600,.8553 ,11519. The electrical conductivity of each material was measured walnut shells 300,600. 4757,7790 and wheat straw 300,600,246 ,722.

Ash content

The ash content was measured and its percentage was found in the following materials wheat straw300,600 and walnut shells300,600.%3056 ,19.4%,3%,3.4%.

Table 2: Chemical properties of the biochars

Chemical properties	Wheat Straw Biochar		Walnut shells Biochar		Composite nano silver with Wheat Straw Biochar		Composite nano silver with Walnut shells Biochar	
	300 °C	600 °C	300 °C	600 °C	300 °C	600 °C	300	600 °C
Temperatue biochar								
C%	53.51	55.31	72.82	85.03	17.76	44.5	28.85	61.18
H%	4.63	4.21	4.5	4.46	2.86	5	2.52	5.02
N%	0.9	0.84	0.88	0.85	0.43	0.76	0.35	0.7
O%	40.95	39.64	21.8	9.66	78.95	49.74	68.28	33.1
pH	8.94	12.00	8.53	11.19				
EC ms m ⁻¹	246	722	4757	7790				
(%) Biochar Yield	45.83%	34.8%	54.37%	66.28				
Ash content	3%	3.4%	19.4%	30.6%				

Conclusions

The biochar was produced from walnut shells with a pyrolysis degree of 600, and had different physical and chemical properties due to the degree of dissolution and the material of its composition. It also had wide porosity and a large surface area, SEM confirms, where the surface

and average volume were different at 28.134 nm. Silver oxide production. In addition, there is a compound that has the characteristics and shape of a sheet, with the oxide in the middle of the band and the average nano size is 216 nanometers, and in elemental analysis the percentage of C was 85.03%, O 9.66%, H% 4.46, and the compound C% was 61.18, H% 5.02, 33.1%. It was good at adsorption of cadmium from aggregate with water.

References

- [1] 1. Kookana RS, Sarmah AK, Van Zwieten L, Krull E, Singh B. Biochar application to soil: agronomic and environmental benefits and unintended consequences. *Advances in agronomy*. 2011;112:103-43.
- [2] 2. Sharma RK, Wooten JB, Baliga VL, Lin X, Chan WG, Hajaligol MR. Characterization of chars from pyrolysis of lignin. *Fuel*. 2004;83(11-12):1469-82.
- [3] 3. Aydin S, Denek N. The effect of fermented lactic acid juice prepared with different levels of sucrose and incubation times on the alfalfa silage quality. *Harran Üniversitesi Veteriner Fakültesi Dergisi*. 2019;8(1):44-51.
- [4] 4. Fahmi AH, Jol H, Singh D. Physical modification of biochar to expose the inner pores and their functional groups to enhance lead adsorption. *RSC advances*. 2018;8(67):38270-80.
- [5] 5. Lakshmi S. Mohana et al. Antipyretic Activity of Pavetta indica Linn.(Rubiaceae) Leaf Extract ...; 2009.
- [6] 6. Ahmed S, Ahmad M, Swami BL, Ikram S. Green synthesis of silver nanoparticles using Azadirachta indica aqueous leaf extract. *Journal of radiation research and applied sciences*. 2016;9(1):1-7.
- [7] 7. Al-Saleh MH. Clay/carbon nanotube hybrid mixture to reduce the electrical percolation threshold of polymer nanocomposites. *Composites Science and Technology*. 2017;149:34-40.
- [8] 8. Savova D, Apak E, Ekinçi E, Yardim F, Petrov N, Budinova T, et al. Biomass conversion to carbon adsorbents and gas. *Biomass and Bioenergy*. 2001;21(2):133-42.
- [9] 9. Song W, Guo M. Quality variations of poultry litter biochar generated at different pyrolysis temperatures. *Journal of analytical and applied pyrolysis*. 2012;94:138-45.
- [10] 10. McGrath SP, Cunliffe CH. A simplified method for the extraction of the metals Fe, Zn, Cu, Ni, Cd, Pb, Cr, Co and Mn from soils and sewage sludges. *Journal of the Science of Food and Agriculture*. 1985;36(9):794-8.
- [11] 11. Shaffiey SF, Shapoori M, Bozorgnia A, Ahmadi M. Synthesis and evaluation of bactericidal properties of CuO nanoparticles against *Aeromonas hydrophila*. *Nanomedicine Journal*. 2014;1(3):198-204.
- [12] 12. Bagheri S, Chandrappa K, Hamid S. Facile synthesis of nano-sized ZnO by direct precipitation method. *Der Pharma Chemica*. 2013;5(3):265-70.
- [13] 13. Jyoti K, Baunthiyal M, Singh A. Characterization of silver nanoparticles synthesized using *Urtica dioica* Linn. leaves and their synergistic effects with antibiotics. *Journal of Radiation Research and Applied Sciences*. 2016;9(3):217-27.

- [14] 14. Imam T, Capareda S. Characterization of bio-oil, syn-gas and bio-char from switchgrass pyrolysis at various temperatures. *Journal of Analytical and Applied Pyrolysis*. 2012;93:170-7.
- [15] 15. Harvey OR, Herbert BE, Kuo L-J, Louchouart P. Generalized two-dimensional perturbation correlation infrared spectroscopy reveals mechanisms for the development of surface charge and recalcitrance in plant-derived biochars. *Environmental science & technology*. 2012;46(19):10641-50.
- [16] 16. Baer DR, Gaspar DJ, Nachimuthu P, Techane SD, Castner DG. Application of surface chemical analysis tools for characterization of nanoparticles. *Analytical and bioanalytical chemistry*. 2010;396:983-1002.
- [17] 17. Claoston N, Samsuri A, Ahmad Husni M, Mohd Amran M. Effects of pyrolysis temperature on the physicochemical properties of empty fruit bunch and rice husk biochars. *Waste Management & Research*. 2014;32(4):331-9.
- [18] 18. Kim KH, Kim J-Y, Cho T-S, Choi JW. Influence of pyrolysis temperature on physicochemical properties of biochar obtained from the fast pyrolysis of pitch pine (*Pinus rigida*). *Bioresource technology*. 2012;118:158-62.
- [19] 19. Fellet G, Marmiroli M, Marchiol L. Elements uptake by metal accumulator species grown on mine tailings amended with three types of biochar. *Science of the Total Environment*. 2014;468:598-608.
- [20] 20. Dedovic, N., Igetic, S., Janic, T., Matic-Kekic, S., Ponjican., O., Tomic., M., et al. (2012). Efficiency of Small Scale Manually Fed Boilers -Mathematical Models. *Energies* 5, 1470–1489
- [21] 21. Li, J., Lin, H., Zhu, K., and Zhang, H. (2017). Degradation of Acid Orange 7 Using Peroxymonosulfate Catalyzed by Granulated Activated Carbon and Enhanced by Electrolysis. *Chemosphere* 188, 139–147
- [22] 22. Kaushal, I., Saharan, P., Kumar, V., Sharma, A. K., and Umar, A. (2019). Superb Sono-Adsorption and Energy Storage Potential of Multifunctional Ag-Biochar Composite. *J. Alloys Compd.* 785, 240–249.
- [23] 23. Singh, P., Sarswat, A., Pittman, C. U., Mlsna, T., and Mohan, D. (2020). Sustainable Low-Concentration Arsenite [As(III)] Removal in Single and Multicomponent Systems Using Hybrid Iron Oxide-Biochar Nanocomposite Adsorbents-A Mechanistic Study. *ACS Omega* 5 (6), 2575–2593.
- [24] 24. Dhas NA, Raj CP, Gedanken A. Synthesis, characterization, and properties of metallic copper nanoparticles. *Chemistry of materials*. 1998;10(5):1446-52.
- [25] 25. Medyńska-Juraszek A, Álvarez ML, Białowiec A, Jerzykiewicz M (2021) Characterization and sodium cations sorption capacity of chemically modified biochars produced from agricultural and forestry wastes. *Materials* 14:4714–53.
- [26] 26. Liang H, Chen L, Liu G, Zheng H (2016) Surface morphology properties of biochars produced from different feedstocks. In *Proceedings of the 2016 International Conference on Civil, Transportation and Environment*, vol 210. <https://doi.org/10.2991/iccte-16.2016.54>.

- [27] 27. Shi W, Ju Y, Bian R, Li L, Joseph S, Mitchell DR et al (2020) Biochar bound urea boosts plant growth and reduces nitrogen leaching. *Sci Total Environ* 701:134424-55.
- [28] 28. Bian R, Joseph S, Cui L, Pan G, Li L, Liu X et al (2014) A three-year experiment confirms continuous immobilization of cadmium and lead in contaminated paddy field with biochar amendment. *J Hazard Mater* 272:121-128
- [29] 29. Chen, Y.; An, D.; Sun, S.; Gao, J.; Qian, L. Reduction and removal of chromium VI in water by powdered activated carbon. *Materials* 2018, 11, 269.
- [30] 30. Georgieva VG, Gonsalvesh L, Tavlieva M (2020) Thermodynamics and kinetics of the removal of nickel (II) ions from aqueous solutions by biochar adsorbent made from agro-waste walnut shells. *J Mol Liq* 312:112788.
- [31] 31. Wang B, Gao B, Wan Y (2018) Entrapment of ball-milled biochar in Ca-alginate beads for the removal of aqueous Cd(II). *J Ind Eng Chem* 61:161-168